Int. J. Heat Mass Transfer. Vol. 26, No. 3, pp. 411–424, 1983
Printed in Great Britain

0017-9310/83/030411-14 $03.00/0
Pergamon Press Ltd.

CONTINUUM EQUATIONS FOR THE PREDICTION OF SHELL-SIDE FLOW AND TEMPERATURE PATTERNS IN HEAT EXCHANGERS

WOUT ZIJL† and HAN DE BRUIJN
B.V. Neratoom, Thermal-Hydraulics Group, Technical Department, P.O. Box 93244, 2509 AE Den Haag, The Netherlands

(*Received* 30 *November* 1981)

Abstract—The so-called fluid–tube continuum approach to describe the thermal-hydraulic performance of heat exchangers is critically reviewed. Special attention is given to the correct formulation of the boundary conditions, and a derivation of the equations starting from basic principles is presented. The resulting linear system of partial differential equations, a Laplace equation and two linear convection equations, is solved numerically by a finite element approximation method based on the least squares minimum principle. Finally, the numerical results are compared with experimental data. The agreement is good.

NOMENCLATURE

A_{ij}, approximation matrix;
c_p, specific heat at constant pressure [J kg^{-1} K^{-1}];
$\boldsymbol{D}$, deformation tensor [s^{-1}];
DDX_{ij}, DDY_{ij}, differentiation matrices [m^{-1}];
E_{ij}, element matrix;
$\mathbf{F}$, force applied on fluid element [N];
$\mathbf{g}$, gravitational acceleration [m s^{-2}];
h_i, scale factors in orthogonal curvilinear co-ordinate system;
h_{loc}, local heat transfer coefficient [W m^{-2} K^{-1}];
H, volumetric heat transfer coefficient [W m^{-3} K^{-1}];
J_v, viscous energy transport term [W];
k, kinetic and viscous energy loss factor [Pa s^2];
K, energy loss factor per unit mass, friction factor per unit length [m^{-1}];
$\boldsymbol{m}$, virtual mass tensor [kg];
$\boldsymbol{M}$, virtual mass tensor per unit mass;
$\mathbf{n}$, unit vector normal to boundary;
N_i, shape functions;
p, pressure [Pa];
$\mathbf{q}$, position vector of moving fluid element [m];
$\mathbf{Q}$, continuously distributed force term per unit mass [m s^{-2}];
r, residual;
r, radial coordinate [m];
$\mathbf{r}$, position vector [m];
R, $K/|\mathbf{v}|^{1/5}$ [m$^{-4/5}$ s$^{-1/5}$];
S, continuously distributed heat source term per unit volume [W m^{-3}];
S_{ij}, system matrix;
t, time [s];
T, shell-side temperature [K];
T_k, kinetic energy of fluid element [J];
u, shell-side radial velocity [m s^{-1}];
v, shell-side axial velocity [m s^{-1}];
$\mathbf{v}$, shell-side velocity [m s^{-1}];
w, tube-side velocity [m s^{-1}];
W_K, kinematical vorticity number;
z, axial co-ordinate [m].

Greek symbols

γ, shell-side porosity;
γ^1, tube-side porosity;
η, dynamic viscosity [Pa s];
η, local co-ordinate (radial);
θ, tube-side temperature [K];
λ, thermal conductivity [W m^{-1} K^{-1}];
ξ, local co-ordinate (axial);
ξ_i, co-ordinates in orthogonal curvilinear system [m];
ρ, density [kg m^{-3}];
ϕ, approximation;
ϕ_v, viscous dissipation term [W];
ω, vorticity divided by porosity [s^{-1}].

Superscripts

$\bar{}$, mean value;
*, liquid volume, in contrast to liquid–tube volume;
$\dot{}$, motional time derivative;
p, integration point index.

Subscripts

p, integration point index.

Del operators in Cartesian co-ordinates

$$(\nabla\phi)_i = (\text{grad }\phi)_i = \frac{\partial\phi}{\partial x_i}, \quad \text{gradient};$$

$$\nabla\cdot\mathbf{A} = \text{div }\mathbf{A} = \frac{\partial A_j}{\partial x_j}, \quad \text{divergence (1)};$$

$$(\nabla\times\mathbf{A})_i = (\text{curl }A)_i = \varepsilon_{ijk}\frac{\partial A_k}{\partial x_j}, \quad \text{curl (2)};$$

$$(\nabla\mathbf{A})_{ij} = \frac{\partial A_j}{\partial x_i}, \quad \text{gradient tensor};$$

$$(\mathbf{A}\nabla)_{ij} = \frac{\partial A_i}{\partial x_j}, \quad \text{transposed gradient tensor};$$

† Present address: Ground-Water Survey TNO, PO Box 285, 2600 AG Delft, The Netherlands.

$$\left.\begin{aligned}\mathbf{v}\cdot\nabla\phi &= v_j\frac{\partial\phi}{\partial x_j},\\ (\mathbf{v}\cdot\nabla\mathbf{A})_i &= v_j\frac{\partial A_i}{\partial x_j},\end{aligned}\right\}\ \text{convective time derivatives;}$$

$$\frac{\partial\phi}{\partial t},\left(\frac{\partial\mathbf{A}}{\partial t}\right)_i=\frac{\partial A_i}{\partial t},\quad\text{local time derivatives;}$$

$$\left.\begin{aligned}\dot{\phi}&=\frac{\mathrm{D}\phi}{\mathrm{D}t}=\frac{\partial\phi}{\partial t}+\mathbf{v}\cdot\nabla\phi,\\ \dot{\mathbf{A}}&=\frac{\mathrm{D}\mathbf{A}}{\mathrm{D}t}=\frac{\partial\mathbf{A}}{\partial t}+\mathbf{v}\cdot\nabla\mathbf{A},\end{aligned}\right\}\ \text{motional time derivative;}$$

$$\left.\begin{aligned}\nabla^2\phi&=\nabla\cdot(\nabla\phi)=\frac{\partial}{\partial x_j}\left(\frac{\partial\phi}{\partial x_j}\right),\\ (\nabla^2\mathbf{A})_i&=[\nabla(\nabla\cdot\mathbf{A})-\nabla\times(\nabla\times\mathbf{A})]_i\\ &=\frac{\partial}{\partial x_j}\left(\frac{\partial A_i}{\partial x_j}\right),\end{aligned}\right\}\ \text{Laplacians;}$$

$$\nabla\mathbf{A}=\tfrac{1}{2}(\nabla\mathbf{A}+\mathbf{A}\nabla)+\tfrac{1}{2}\begin{pmatrix}0 & (\nabla\times\mathbf{A})_3 & -(\nabla\times\mathbf{A})_2\\ -(\nabla\times\mathbf{A})_3 & 0 & (\nabla\times\mathbf{A})_1\\ (\nabla\times\mathbf{A})_2 & -(\nabla\times\mathbf{A})_1 & 0\end{pmatrix},$$

Gibbsian decomposition;

(1) two repeated indices denote summation over these indices;

(2) $$\varepsilon_{ijk}=\begin{cases}0 & \text{if } i=j \text{ or } i=k \text{ or } j=k,\\ +1 & \text{if } (i,j,k)=(1,2,3)\\ & \text{or } (2,3,1) \text{ or } (3,1,2),\\ -1 & \text{if } (i,j,k)=(2,1,3)\\ & \text{or } (1,3,2) \text{ or } (3,2,1),\end{cases}$$

Levi–Civita tensor;

1. INTRODUCTION

ESPECIALLY when heat exchangers and steam generators for Liquid Metal cooled Fast Breeder Reactors (LMFBR) are considered, a high integrity is required and, to avoid unacceptable thermal stresses, a thorough knowledge of the 3-dim. temperature distribution is necessary for both design and licensing purposes.

In Fig. 1, an example of a straight-tube shell-and-tube heat exchanger is presented. The flow distribution on the shell side of a shell-and-tube heat exchanger or steam generator has a significant influence on the temperature distribution across the tube bundle and, consequently, on the thermal stresses caused by the temperature gradients. For that reason, this paper will mainly be concerned with the equations describing flow.

The equations to be solved are well established; they are the classical partial differential equations expressing conservation of mass, linear momentum and energy for a Newtonian fluid. To simplify the analysis, it will be assumed that the density, ρ, the viscosity, η, and the conductivity, λ, are constants. In this way natural convection need not be considered.

Under these assumptions, the basic equations describing the fluid motion are independent of the energy equation and they reduce to the well known requirement of divergence-free flow and to the Navier–Stokes equations

$$\nabla\cdot\mathbf{v}=0, \tag{1}$$

$$\frac{\mathrm{D}\mathbf{v}}{\mathrm{D}t}=\nabla\left(\mathbf{g}\cdot\mathbf{r}-\frac{p}{\rho}\right)+\frac{\eta}{\rho}\nabla^2\mathbf{v}. \tag{2}$$

(See ref. [1] for a thorough investigation of the mathematical properties of the Navier–Stokes equations.)

To obtain a well-posed partial differential problem, initial and boundary conditions must be prescribed for the Navier–Stokes equations. The initial condition is that $\mathbf{v}(\mathbf{r},0)$ must be prescribed at time $t=0$, and a boundary condition at a boundary completely enclosing the fluid is that the velocity, $\mathbf{v}$, may be prescribed for all times $t>0$. For the tube bundle under consideration, this means that $\mathbf{v}=\mathbf{0}$ must also be prescribed at the boundaries of the rigid tubes. It is worthwhile to emphasize the fact that the use of the above-mentioned initial and boundary conditions excludes the prescription of the pressure, p, as an initial or boundary condition [2].

From the energy equation and the Navier–Stokes equations, an equation for the temperature, T, can be derived.

$$\rho c_p\frac{\mathrm{D}T}{\mathrm{D}t}=\lambda\nabla^2T+2\eta\boldsymbol{D}:\boldsymbol{D}. \tag{3}$$

In equation (3) $\boldsymbol{D}=(\nabla\mathbf{v}+\mathbf{v}\nabla)/2$ is the deformation tensor, and the heat production by radiation has been neglected. (For a detailed derivation of both the Navier–Stokes equations and the temperature equation see ref. [3].)

Although the equations and boundary conditions needed for the prediction of the shell-side flow pattern are well-established, it is, however, also a well-known fact that the Navier–Stokes equations are difficult to solve. Even for simple geometries, analytical and numerical solutions can only be obtained for relatively low Reynolds numbers. Furthermore, the very simple, from a mathematical point of view, equations describing incompressible, irrotational flow, i.e.

$$\nabla\cdot\mathbf{v}=0, \tag{1}$$

$$\nabla\times\mathbf{v}=\mathbf{0}, \tag{4}$$

can hardly be solved if a tube bundle is present, due to the very complex geometry. The requirement that $\mathbf{n}\cdot\mathbf{v}=0$ at all tube walls is prohibitive.

Due to the reasons mentioned above, a solution of the Navier–Stokes equations is completely out of the question and approximations must be introduced. Several investigators have attempted to describe the

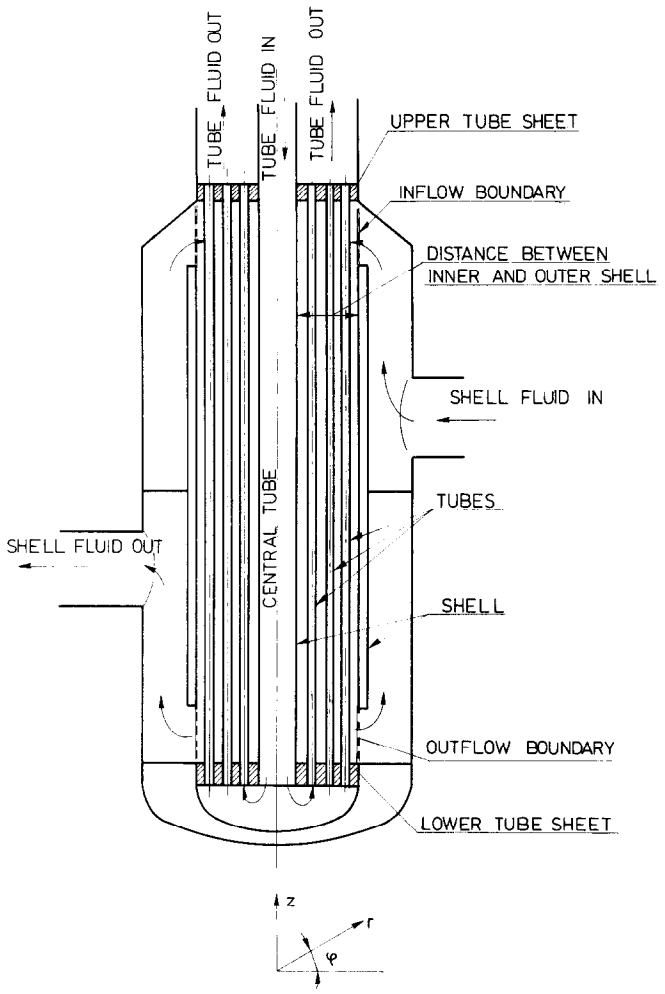

FIG. 1. Example of straight-tube shell-and-tube heat exchanger.

shell-side flow distribution approximately by partial differential equations describing a so-called fluid–tube continuum [4–7]. In the Appendix a derivation of these equations will be presented. The equations describing motion in the fluid–tube continuum are shown to have essentially the same character as the well-known Euler equations describing inviscid fluid dynamics; the only difference being a porosity factor, γ, representing the ratio of the volume occupied by the fluid and the total volume, and a continuously distributed force term, $\mathbf{Q}$, accounting for the resistance of the tubes. Also, the equation describing the temperature in a fluid–tube continuum contains a continuously distributed heat source term, S, accounting for the heat transport to the tubes.

In the next section, the fluid–tube continuum equations are postulated and worked out to a suitable basis for numerical treatment. In Section 3, the finite element method, used to solve the resulting equations, is explained briefly. In Section 4, numerical results for an intermediate heat exchanger designed for a LMFBR plant are shown and compared with experimental data.

Finally, in the Appendix, a derivation of the fluid–tube continuum equations will be presented starting from the fundamental conservation equations (1)–(3).

2. FLUID–TUBE CONTINUUM EQUATIONS AND BOUNDARY CONDITIONS

Starting from the fundamental conservation equations (1)–(3), the fluid–tube continuum equations are derived in the Appendix, the equations resulting being [4–7]

$$\nabla\cdot(\gamma\bar{\mathbf{v}}) = 0, \tag{5}$$

$$\frac{\mathrm{D}\bar{\mathbf{v}}}{\mathrm{D}t} = \nabla\left(\mathbf{g}\cdot\mathbf{r} - \frac{\bar{p}}{\rho}\right) + \mathbf{Q} \tag{6}$$

and

$$\rho c_p \frac{\mathrm{D}\bar{T}}{\mathrm{D}t} = S. \tag{7}$$

In equations (5)–(7), $\bar{\mathbf{v}}$ is the mean velocity, $\bar{p}$ the mean pressure, and $\bar{T}$ the mean temperature. The force

distribution, $\mathbf{Q}$, and the heat source distribution, S, are additional unknowns for which additional expressions, either coming from experimental data or from analytical solutions of relatively simple problems, must be found. In all previous analyses [4–7], only the steady-state expression for $\mathbf{Q}$ was applied, which leads to physically doubtful results when transient phenomena are considered. In the Appendix, a possibility of modifying $\mathbf{Q}$ in such a way that unsteady phenomena can be described will be proposed.

2.1. *The flow field*

In classical (inviscid) fluid dynamics, it is customary to eliminate the pressure from equation (6) by taking the curl of it and using equation (5), resulting in an expression describing the convection of vorticity divided by the porosity, $\bar{\boldsymbol{\omega}} = (\nabla \times \bar{\mathbf{v}})/\gamma$,

$$\frac{\mathrm{D}\bar{\boldsymbol{\omega}}}{\mathrm{D}t} = \bar{\boldsymbol{\omega}} \cdot \bar{\mathbf{D}} + \frac{1}{\gamma} \nabla \times \mathbf{Q} \tag{8}$$

where $\bar{\mathbf{D}} = (\nabla\bar{\mathbf{v}} + \bar{\mathbf{v}}\nabla)/2$ is the so-called deformation tensor. If $\nabla \times \mathbf{Q} = \mathbf{0}$, equation (8) is exactly equivalent to the Helmholtz form of the Euler equations [23].

The physical meaning of the so-called generalized Helmholtz equation (8) is that the vorticity of a piece of fluid (divided by the porosity) changes with a rate $\bar{\boldsymbol{\omega}} \cdot \bar{\mathbf{D}} + (\nabla \times \mathbf{Q})/\gamma$ during the motion of this piece of fluid along its streamline. A consequence of this is that the vorticity must be prescribed both as an initial condition and as a boundary condition on the inflow opening. If these latter conditions represent zero vorticity and if $\nabla \times \mathbf{Q} \propto -\bar{\boldsymbol{\omega}}$, it follows from equation (8) that $\nabla \times \bar{\mathbf{v}} = \mathbf{0}$ in the complete flow field. In this case, equations (5) and (4) must be solved for $\bar{\mathbf{v}}$, however, without boundary conditions on the individual tubes, i.e. for a relatively simple geometry. In general, the condition $\nabla \times \mathbf{Q} \propto -\bar{\boldsymbol{\omega}}$ does not hold and, as a consequence, vorticity is produced in the flow field. As a matter of course, this vorticity, $\gamma\bar{\boldsymbol{\omega}}$, must be solenoidal, i.e. $\nabla \cdot (\gamma\bar{\boldsymbol{\omega}}) = 0$, since only in that case can the vorticity be interpreted as $\nabla \times \bar{\mathbf{v}}$.

From equations (5) and (8) it can be derived that if the condition $\nabla \cdot (\gamma\bar{\boldsymbol{\omega}}) = 0$ is prescribed at the inflow boundary then $\gamma\bar{\boldsymbol{\omega}}$ is automatically solenoidal in the complete flow field (provided, of course, that at $t = 0$, $\gamma\bar{\boldsymbol{\omega}}(\mathbf{r}, 0)$ is solenoidal).

In the following discussion, the conditions for $\mathbf{Q}$ under which the vorticity, $\gamma\bar{\boldsymbol{\omega}}$, may be taken equal to zero at the inflow boundary will be sought. For that purpose, an orthogonal curvilinear co-ordinate system with co-ordinates $\mathbf{r} = (\xi_1, \xi_2, \xi_3)$ will be considered. In this co-ordinate system, ξ_3 is the co-ordinate in the direction of the normal unit vector, $\mathbf{n}$, at the inflow boundary, and ξ_1 and ξ_2 are co-ordinates parallel to that boundary [8]. Under the condition that $\bar{\boldsymbol{\omega}} = \mathbf{0}$ at the inflow boundary, the condition $\nabla \cdot (\gamma\bar{\boldsymbol{\omega}}) = 0$ at that boundary can be written as

$$\nabla \cdot (\gamma\bar{\boldsymbol{\omega}}) = \frac{\gamma}{h_3} \frac{\partial \bar{\omega}_3}{\partial \xi_3} = 0.$$

The same condition includes, for the ξ_3-component of equation (8),

$$\frac{\bar{v}_3}{h_3} \frac{\partial \bar{\omega}_3}{\partial \xi_3} = \frac{1}{\gamma h_1 h_2} \left(\frac{\partial Q_2 h_2}{\partial \xi_1} - \frac{\partial Q_1 h_1}{\partial \xi_2} \right).$$

Since, by definition, $\bar{v}_3 = \mathbf{n} \cdot \bar{\mathbf{v}} \neq 0$ at the inflow boundary, both equations can be combined to give

$$\frac{1}{h_1 h_2} \left(\frac{\partial Q_2 h_2}{\partial \xi_1} - \frac{\partial Q_1 h_1}{\partial \xi_2} \right) = \mathbf{n} \cdot \nabla \times \mathbf{Q} = 0.$$

Consequently, the inflow boundary condition $\boldsymbol{\omega} = \mathbf{0}$ may be applied only if $\mathbf{n} \cdot \nabla \times \mathbf{Q} = 0$ at the inflow boundary. In the following discussions, this latter condition will always be assumed to hold.

The difference between the Navier–Stokes equations and the Euler equations is the absence of the second order term $(\eta/\rho)\nabla^2\mathbf{v}$ in the Euler equations. One of the consequences of this absence is a simplification of the boundary conditions. Instead of shell boundary conditions for the three components of $\mathbf{v}$ for the Navier–Stokes equations, the boundary condition $\mathbf{v} \cdot \mathbf{n} = 0$ holds for the Euler equations at the rigid solid shell. This latter mathematical feature makes Euler-like equations especially well-suited for the description of a fluid–tube continuum, in contrast to Navier–Stokes-like equations, as will be shown in the following discussion.

From a physical point of view, the boundary conditions in a fluid–tube continuum are that no fluid is flowing out of the impermeable shell, i.e. $\bar{\mathbf{v}} \cdot \mathbf{n} = 0$ on the shell. Of course, in a fluid–tube continuum no boundary conditions may be prescribed on the tubes; a mean volumetric flow rate of fluid is passing across a unit area containing tubes, and the local fluid velocity, as it passes through the clearances between the tubes, will not be considered. Additional boundary conditions, e.g. for the velocity components parallel to the wall, for the so-called turbulent tangential stress, or for the vorticity, may not be prescribed, since in that case there is no reason why the same condition is not applied at the boundaries of the individual tubes. Consequently, from a physical point of view, the boundary conditions in a fluid–tube continuum approximation have an Euler-like character.

The difference between the present study and the earlier treatments [4–7] is that the latter authors did not make use of the advantages of the Euler-like character of the equations, whereas in this paper these advantages will be fully exploited. In the following part of this section, equation (8) will further be simplified by making use of an expression for $\mathbf{Q}$.

2.2. *Irrotational flow*

In the Appendix it is proved that

$$\mathbf{Q} = -\tfrac{1}{2}K|\bar{\mathbf{v}}|\bar{\mathbf{v}} - \boldsymbol{M} \cdot \frac{\partial \mathbf{v}}{\partial t} + \frac{\partial \mathbf{v}}{\partial t} \tag{9}$$

where K is a positive friction factor accounting for the steady viscous drag and the pressure drop in the wakes

at the tubes. M is a positive definite virtual mass tensor accounting for the fact that immersion of tubes in the liquid increases the kinetic energy of the motion with respect to the kinetic energy without tubes (see Kelvin's theorem in ref. [9]).

From the discussion presented above it is clear that the value of $\nabla \times \mathbf{Q}$ plays an important part, and it is given by

$$\nabla \times \mathbf{Q} = -\tfrac{1}{2}K|\bar{\mathbf{v}}|\Big[\gamma\bar{\boldsymbol{\omega}} - \tfrac{4}{5}\bar{\mathbf{v}} \times \nabla \ln|\bar{\mathbf{v}}| - \bar{\mathbf{v}} \times \left(\frac{\partial \ln R}{\partial \bar{\mathbf{v}}} \cdot \nabla\bar{\mathbf{v}}\right) - \bar{\mathbf{v}} \times \frac{\partial \ln R}{\partial \mathbf{r}}\Big] + \frac{\partial \bar{\boldsymbol{\omega}}}{\partial t} - \nabla \times \left(\boldsymbol{M} \cdot \frac{\partial \bar{\mathbf{v}}}{\partial t}\right). \tag{10}$$

It has been assumed, in agreement with experimental data for turbulent flow in tube banks, that $K = R/|\bar{\mathbf{v}}|^{1/5}$, where $R = R(\mathbf{r}, \bar{\mathbf{v}})$ is a function of $\mathbf{r}$ and of the direction of the flow velocity only (i.e. $\bar{\mathbf{v}} \cdot (\partial R/\partial \bar{\mathbf{v}}) = 0$) [10].

To simplify equation (10), a steady-state situation will be considered, i.e. $\partial \bar{\mathbf{v}}/\partial t = \mathbf{0}$. Furthermore, a homogeneous force distribution will be considered, i.e. $\partial R/\partial \mathbf{r} = \nabla R = \mathbf{0}$. Under these assumptions, equation (10) simplifies to

$$\frac{1}{\gamma}\nabla \times \mathbf{Q} = -\tfrac{7}{10}K|\bar{\mathbf{v}}|\Big[\bar{\boldsymbol{\omega}} - \tfrac{2}{7}(\mathbf{e}\cdot\bar{\boldsymbol{\omega}})\mathbf{e} + \tfrac{5}{14}(\bar{\mathbf{v}}\cdot\bar{\boldsymbol{\omega}})\frac{\partial \ln R}{\partial \bar{\mathbf{v}}} - \frac{4}{7\gamma}\mathbf{e} \times (\mathbf{e}\cdot\bar{\boldsymbol{D}}) - \frac{5}{7\gamma}\bar{\mathbf{v}} \times \left(\frac{\partial \ln R}{\partial \bar{\mathbf{v}}} \cdot \bar{\boldsymbol{D}}\right)\Big]. \tag{11}$$

In equation (11) $\mathbf{e} = \bar{\mathbf{v}}/|\bar{\mathbf{v}}|$. Use has been made of the vector relation

$$\bar{\mathbf{v}} \cdot \nabla\bar{\mathbf{v}} = \nabla\tfrac{1}{2}|\bar{\mathbf{v}}|^2 + \gamma\bar{\boldsymbol{\omega}} \times \bar{\mathbf{v}}$$

and of the Gibbs decomposition theorem for $\nabla\bar{\mathbf{v}}$

$$\mathbf{a} \cdot \nabla\bar{\mathbf{v}} = \mathbf{a} \cdot \bar{\boldsymbol{D}} + (\gamma\bar{\boldsymbol{\omega}} \times \mathbf{a})/2,$$

with $\mathbf{a} = \mathbf{e}$ and $\mathbf{a} = \partial \ln R/\partial \mathbf{v}$, respectively. It is important to note here that the deformation tensor, $\bar{\boldsymbol{D}} = (\nabla\bar{\mathbf{v}} + \bar{\mathbf{v}}\nabla)/2$, at a point depends only on the irrotational part of the local velocity field and not directly on the local value of the vorticity, $\gamma\bar{\boldsymbol{\omega}}$ (ref. [11], Ch. 34). Consequently, equation (11) represents a splitting of $\nabla \times \mathbf{Q}$ into parts depending either on only irrotational or on only rotational modes of fluid motion.

When a 2-dim. flow or an axially symmetric flow without circulation around the axis of symmetry is considered, $\bar{\mathbf{v}} \cdot \bar{\boldsymbol{\omega}} = 0$ holds. In addition, $\bar{\boldsymbol{\omega}} \cdot \bar{\boldsymbol{D}}$ in equation (8) is equal to zero when a 2-dim. flow is considered and the term $(\mathrm{D}\bar{\boldsymbol{\omega}}/\mathrm{D}t) - \bar{\boldsymbol{\omega}} \cdot \bar{\boldsymbol{D}}$ in equation (8) is equal to $r(\mathrm{D}/\mathrm{D}t)(\omega/r)$ when an axially symmetric flow without circulation around the axis of symmetry is considered. Under these conditions combination of equations (8) and (11) result in

$$r^n \frac{\mathrm{D}}{\mathrm{D}t}\left(\frac{\omega}{r^n}\right) = -\tfrac{7}{10}K|\bar{\mathbf{v}}|\Big[\bar{\boldsymbol{\omega}} - \frac{4}{7\gamma}\mathbf{e} \times (\mathbf{e}\cdot\bar{\boldsymbol{D}}) - \frac{5}{7\gamma}\bar{\mathbf{v}} \times \left(\frac{\partial \ln R}{\partial \bar{\mathbf{v}}} \cdot \bar{\boldsymbol{D}}\right)\Big] \tag{12}$$

where $n = 0$ for 2-dim. flow and $n = 1$ for axially symmetric flow without circulation around the axis of symmetry.

At the inflow boundary, $\bar{\boldsymbol{\omega}} = \mathbf{0}$, and moving with a piece of fluid along its streamline, it is observed from the relaxation character of equation (12) that $\gamma\bar{\boldsymbol{\omega}}$ tends from zero to an asymptotic value of

$$\gamma\bar{\boldsymbol{\omega}} = \left[4\mathbf{e} \times (\mathbf{e}\cdot\bar{\boldsymbol{D}}) + 5\bar{\mathbf{v}} \times \left(\frac{\partial \ln R}{\partial \bar{\mathbf{v}}} \cdot \bar{\boldsymbol{D}}\right)\right]/7 = \gamma\mathbf{b}$$

in a characteristic time interval $\Delta t \simeq (2 \times 10)/(7K|\bar{\mathbf{v}}|)$. During that time interval, the piece of fluid under consideration has travelled a characteristic distance $\Delta L \simeq |\bar{\mathbf{v}}|\Delta t = 20/(7K)$.

At a distance of order of magnitude L from the inflow boundary, where L is the distance between inner and outer shell, the flow becomes parallel to the shells. In a parallel flow region is

$$\bar{\mathbf{v}} \times \left(\frac{\partial \ln R}{\partial \bar{\mathbf{v}}} \cdot \bar{\boldsymbol{D}}\right) = 0, \quad \mathbf{e} \times (\mathbf{e}\cdot\bar{\boldsymbol{D}}) = -\gamma\bar{\boldsymbol{\omega}}/2$$

and

$$\gamma\boldsymbol{\omega} = (0, 0, -\partial v/\partial r).$$

Substitution of these values in equation (12) shows that in a parallel flow region where $\partial\gamma/\partial r = 0$ or $\partial\gamma/\partial z = 0$ the flow is irrotational. An order of magnitude estimation results in

$$|\mathbf{e} \times (\mathbf{e}\cdot\bar{\boldsymbol{D}})| \lesssim (\tfrac{1}{2}\bar{\boldsymbol{D}} : \bar{\boldsymbol{D}})^{1/2}$$

and

$$\left|\bar{\mathbf{v}} \times \left(\frac{\partial \ln R}{\partial \bar{\mathbf{v}}} \cdot \bar{\boldsymbol{D}}\right)\right| \lesssim \left|\ln \frac{R_\perp}{R_\parallel}\right| (\tfrac{1}{2}\bar{\boldsymbol{D}} : \bar{\boldsymbol{D}})^{1/2},$$

near the inflow boundary. At a distance L from this boundary these terms are equal to zero, and at a distance $L/2$ these terms have half the value at the inflow opening. Here $R_\perp$ and $R_\parallel$ are the friction factors for flow normal and parallel to the tubes, respectively.

In summary, in a region near the inflow boundary, $\bar{\boldsymbol{\omega}}$ tends from zero at the inflow opening, via a maximum value at a distance of approximately $L/2$ from the inflow boundary to zero at a distance L.

At the location of maximum $|\bar{\boldsymbol{\omega}}|$, $|\mathbf{b}|$ has half the value of its maximum at the inflow opening and, due to the relaxation character of equation (12), the maximum value of $|\bar{\boldsymbol{\omega}}|$ is equal to $\frac{1}{2}(L/\Delta L)|\mathbf{b}|$, or

$$\gamma|\bar{\boldsymbol{\omega}}|_{\max} \lesssim \tfrac{1}{80}KL(\tfrac{1}{2}\bar{\boldsymbol{D}} : \bar{\boldsymbol{D}})^{1/2} \times \left(4^2 + 5^2\left|\ln \frac{K_\perp}{K_\parallel}\right|^2\right)^{1/2} \quad \text{if} \quad KL < 80/7,$$

$$\gamma|\bar{\boldsymbol{\omega}}|_{\max} \lesssim \tfrac{1}{7}(\tfrac{1}{2}\bar{\boldsymbol{D}} : \bar{\boldsymbol{D}})^{1/2} \times \left(4^2 + 5^2\left|\ln \frac{K_\perp}{K_\parallel}\right|^2\right)^{1/2} \quad \text{if} \quad KL > 80/7$$

where the contributions of the two terms have been summed in a RMS sense. In the following discussion, it is accepted that this represents an acceptable approximation for a general 3-dim. flow also.

It follows from a Taylor series expansion and from the Gibbsian decomposition of $\nabla\bar{\mathbf{v}}$ that the velocity at a point $\mathbf{r}+\mathbf{h}$ can be expressed as

$$\bar{\mathbf{v}}(\mathbf{r}+\mathbf{h}) = \bar{\mathbf{v}}(\mathbf{r})+\mathbf{h}\cdot\nabla\bar{\mathbf{v}}+O(h^2)$$
$$= \bar{\mathbf{v}}(\mathbf{r})+\mathbf{h}\cdot\bar{\boldsymbol{D}}+\tfrac{1}{2}\gamma\bar{\boldsymbol{\omega}}\times\mathbf{h}+O(h^2).$$

From this expression, it can be observed that the kinematical effect of vorticity with respect to irrotational modes of motion can be characterized by the ratio $|\gamma\bar{\boldsymbol{\omega}}\times\mathbf{h}|/|2\mathbf{h}\cdot\bar{\boldsymbol{D}}|$, or, since a characterization independent of $\mathbf{h}$ is preferable, by the ratio

$$W_K = \frac{\gamma|\bar{\boldsymbol{\omega}}|}{2(\frac{1}{2}\bar{\boldsymbol{D}}:\bar{\boldsymbol{D}})^{1/2}}$$

where W_K is the so-called kinematical vorticity number (ref. [11], Ch. 56). Finally, it follows from this discussion that, at the place where $|\bar{\boldsymbol{\omega}}|$ has its maximum value, W_K has the following order of magnitude:

$$W_K \gtrsim 0.025KL\left(1+1.56\left|\ln\frac{K_\perp}{K_\parallel}\right|^2\right)^{1/2} \quad \text{if} \quad KL<11.4,$$

$$W_K \gtrsim 0.286\left(1+1.56\left|\ln\frac{K_\perp}{K_\parallel}\right|^2\right)^{1/2} \quad \text{if} \quad KL>11.4.$$

For a tube bank with values of $K=K_\perp=K_\parallel=40\ \mathrm{m}^{-1}$ and $L=0.25$ m, a value of $W_K \gtrsim 25\%$ is found in the flow field at the place where maximum vorticity occurs. Also, if $K_\perp=32\ \mathrm{m}^{-1}$ and $K_\parallel=8\ \mathrm{m}^{-1}$, or if $K_\perp=20\ \mathrm{m}^{-1}$ and $K_\parallel=0.4\ \mathrm{m}^{-1}$, with a mean value for K of $(K_\perp+K_\parallel)/2$, a value of $W_K \gtrsim 25\%$ is found for $L=0.25$. Especially the latter two examples are representative for tube banks in actual heat exchangers. This means that, for practical purposes, the flow may be considered as irrotational, especially since the above-estimated contribution of vorticity to the complete flow field only applies in the relatively small region where vorticity has its maximum value.

For the purpose of reference, note that both for generalized Poiseuille flow and for boundary layer flow along a flat, infinitely extended wall, $W_K=1$, whereas for rigid rotation, $W_K=\infty$.

The conclusion is that for steady forced convection, where natural convection is negligible, the shell-side mean flow pattern in a tube bank may be described by the following simple linear equations:

$$\nabla\cdot(\gamma\bar{\mathbf{v}})=0, \tag{5}$$

$$\nabla\times\bar{\mathbf{v}}=0. \tag{13}$$

Since equation (13) can identically be satisfied by $\bar{\mathbf{v}}=\nabla\bar{\phi}$, equation (5) is equivalent to the Laplace equation, $\nabla\cdot(\gamma\nabla\bar{\phi})=0$, for the velocity potential, $\bar{\phi}$. The advantage of this latter equation is that it can simply be solved numerically with the aid of finite element packages commercially available for applications in structural mechanics [22]. However, in this paper the potential formulation will not be used.

A more accurate calculation to account for the small amount of vorticity in the flow field would not be helpful since it would depend both on the prescribed velocity and vorticity at the inflow-boundary, and on experimentally determined values of $K(\bar{\mathbf{v}})$. The accuracy of these values, in combination with the fluid-tube continuum approximation, is certainly not so good to justify an accuracy better than 20–30% in the calculation of the mean flow velocity field. This conclusion does not hold if baffles are present in the flow field since, in that case, vorticity detaching at the separation line is transported into the flow field by means of convection. Consequently, in that case, a non-zero value for the vorticity must be prescribed as an inflow boundary condition at the line of separation.

2.3. *The temperature fields*

The equation for the steady mean temperature at the shell-side, $\bar{T}$, is given by

$$\gamma\rho c_p\bar{\mathbf{v}}\cdot\nabla\bar{T} = -\gamma^1 H(\bar{T}-\bar{\theta}) \tag{14}$$

and, for straight tubes parallel to the z-axis, the equation for the steady temperature at the tube side, $\bar{\theta}$, is

$$\rho c_p\bar{w}\frac{\partial\bar{\theta}}{\partial z} = H(\bar{T}-\bar{\theta}). \tag{15}$$

In equation (15), γ^1 is the volume fraction of liquid in the tubes. The value of H is given by $4h_{\mathrm{loc}}/D$, where h_{loc} is the local heat transfer coefficient, and D is the inner diameter of the tube (ref. [12] Ch. 13.1; ref. [10], Ch. 3.10).

If unsteady heat transfer is considered, the equations describing heat storage in the tube wall must be considered in addition. However, for the steady heat transport under consideration, all heat coming from the shell-side is transported to the tube-side without accumulation of heat in the tube walls.

The boundary condition for the convection equation (14) is that $\bar{T}$ must be prescribed at the inflow opening only; this is similar to the case discussed earlier for the vorticity convection equation (8). Also, for equation (15), $\bar{\theta}$ must be prescribed at $z=0$. It should be remarked, however, that, in contrast to the momentum equation (6), it does make sense from a physical point of view to include turbulent heat diffusion terms, i.e. a term $\lambda\nabla^2\bar{T}$ in equation (14) and a term $\lambda\partial^2\bar{\theta}/\partial z^2$ in equation (15). For example, if only thermally insulating tubes are present, heat transfer takes place by turbulent diffusion only, and not by heat transport from shell-side to tube-side liquid. If these diffusion terms are present, either $\bar{T}$, or $\partial\bar{T}/\partial n$ or a combination of both must be prescribed at a boundary completely enclosing the temperature field; also, in that case, either $\bar{\theta}$, or $\partial\bar{\theta}/\partial z$ or a combination of both must be prescribed at $z=0$ and at the end of the tubes. In the present study, however, diffusion terms are assumed to be sufficiently small with

respect to the terms representing heat transport from shell-side to tube-side liquid.

3. NUMERICAL APPROXIMATION

In this section, a method by which any set of first-order partial differential equations in two variables can be easily discretized will be applied. This so-called Least Squares Finite Element Method (LSFEM) has already been reported [13, 14], and only a brief summary of the basic philosophy and principles will be presented here.

In contrast to the global interpolation methods [15], LSFEM is a local interpolation method, i.e. the domain of interest is divided into a great number of sub-domains, or finite elements. In these elements, functions are approximated by polynomial expansions interpolating the function values at the interpolation points, or nodes of the element. As an example, take the four-node element in two space dimensions with nodes $j, j = 1, \ldots, 4$, defined by (Fig. 2)

$$(1) = (-\tfrac{1}{2}, -\tfrac{1}{2}); \quad (2) = (+\tfrac{1}{2}, -\tfrac{1}{2}),$$
$$(3) = (-\tfrac{1}{2}, +\tfrac{1}{2}); \quad (4) = (+\tfrac{1}{2}, +\tfrac{1}{2}). \tag{16}$$

To this element, or so-called computational molecule, belongs a 4-dim. vector space spanned by a set of four independent polynomials:

$$\mathbf{l} = (1, \eta, \xi, \eta\xi).$$

In this vector space, an interpolation, ϕ, is defined by

$$\phi = a_1 + a_2\eta + a_3\xi + a_4\eta\xi$$

or

$$\phi = l_i a_i \tag{17}$$

where the well-known summation convention is employed. Substitution of the co-ordinates of the four nodes (16) into the interpolation (17) results in a set of four linear equations

$$a_i = c_{ij}\phi_j$$

or

$$\phi = N_j\phi_j, \tag{18}$$

where $N_j = l_i c_{ij}$ are the shape functions of the finite element. The matrix $(c^{-1})_{ij} = l_j(\eta_i, \xi_i)$ is non-singular. Differentiation of the interpolation, ϕ, with respect to ξ results in

$$\frac{\partial\phi}{\partial\xi} = \frac{\partial N_j}{\partial\xi}\phi_j.$$

Again, the functions $\partial N_j/\partial\xi$ can be expressed as linear combinations of the shape functions

$$\frac{\partial N_j}{\partial\xi} = N_i DDH_{ij}.$$

By substitution of the co-ordinates of the four nodes (16), and by making use of $N_i(\text{node } j) = \delta_{ij}$, the matrix of coefficients, DDK_{ij}, is found to be

$$DDK_{ij} = \frac{\partial N_j}{\partial\xi}(\text{node } i). \tag{19}$$

A similar matrix, DDH_{ij}, is obtained for the differential operator $\partial/\partial\eta$. The matrices DDH_{ij} and DDK_{ij} are the so-called "differentiation matrices" [16, 17] or "derivation matrices" [18].

The four-node molecule (16) is used as a parent-element for a general quadrilateral derived from it by isoparametric mapping [19]

$$x = N_i x_i, \quad y = N_i y_i.$$

Matrix-equivalents, DDX_{ij} and DDY_{ij}, corresponding to differentiations, $\partial/\partial x$ and $\partial/\partial y$, in the (x, y) plane can be found from equation (19) in the following way:

$$DDX_{ij} = \left(\frac{\partial y}{\partial\xi}DDH_{ij} - \frac{\partial y}{\partial\eta}DDK_{ij}\right)/J,$$
$$DDY_{ij} = \left(-\frac{\partial x}{\partial\xi}DDH_{ij} + \frac{\partial x}{\partial\eta}DDK_{ij}\right)/J \tag{20}$$

where J is the Jacobian determinant given by

$$J = \frac{\partial x}{\partial\eta}\frac{\partial y}{\partial\xi} - \frac{\partial x}{\partial\xi}\frac{\partial y}{\partial\eta}.$$

The functions $\partial(x, y)/\partial(\eta, \xi)$ and J are linear in η, ξ, and they can conveniently be evaluated at the element midpoint. In addition, a matrix representation for operators containing functions is needed. If it is required that a product-function, $f\cdot\phi$, lies within the element vector space, then it is obvious that

$$f\cdot\phi = N_i(f\cdot\phi)_i. \tag{21}$$

As a consequence, the elementary function matrices are diagonal, the non-zero elements being the values of the function at the element nodes [13, 14]. When the value of $\phi = N_i\phi_i$ is evaluated at a certain point, p, in the element this is called a projection. Any universal least squares finite element has as many projection points, or integration points, as it has nodes, or interpolation points (Fig. 2). The evaluation of the interpolation polynomials at the projection points is summarized in a matrix, P_{ij}, the so-called projection-matrix

$$P_{ij} = N_j(\text{point } i). \tag{22}$$

The universal matrices DDX_{ij}, DDY_{ij} and P_{ij} are worked out explicitly for a general quadrilateral with

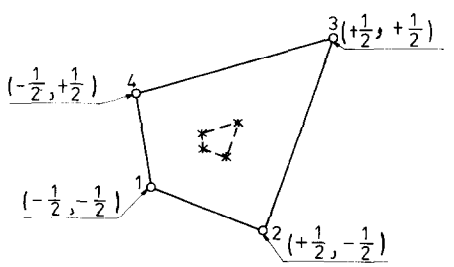

FIG. 2. Four-node computational molecule. ○ Nodal points = interpolation points. * integration points = projection points.

four integration points, and they are coded in a FORTRAN routine with the name QUAD4. Using these universal matrices from QUAD4, it is very simple to construct approximations for the equations, e.g. for the system of equations (5) and (13)–(15). All these approximations are characterized by a relationship of the form

$$r = N_i A_{ij} \phi_j \tag{23}$$

where r is the residual of the equations to be minimized, N_i the appropriate set of shape functions defined by equation (18), ϕ_j the vector of unknowns, and A_{ij} the so-called 'approximation matrix' of the governing equations.

The approximation matrix, A_{ij}, contains all the information of the problem discretized for the element under consideration. To apply the matrix method conveniently, the equations must be presented in a somewhat different form. As an example, for an axially symmetric flow field without circulation around the axis of symmetry, equations (5) and (13) with constant γ can be written as

$$\begin{pmatrix} \frac{\partial}{\partial x} x & x \frac{\partial}{\partial y} \\ -\frac{\partial}{\partial y} & \frac{\partial}{\partial x} \end{pmatrix} \begin{pmatrix} \bar{u} \\ \bar{v} \end{pmatrix} = \begin{pmatrix} 0 \\ 0 \end{pmatrix} \tag{5, 13}$$

where x and y represent the co-ordinates in radial and axial direction respectively, i.e. $x = r$ and $y = z$. The approximation matrix, A_{ij}, can be constructed now, resulting in

$$A_{ij} = \begin{pmatrix} DDX(I,J)*X(J) & X(I)*DDY(I,J) \\ -DDY(I,J) & DDX(I,J) \end{pmatrix},$$

with no summation over equal indices. In a similar way, equations (14) and (15) for the mean temperature fields, and equations (6) and (9) for the mean pressure field can be transformed into approximation matrices.

The residual, r, of the approximating equations specified for a finite element like equations (11), is given by equation (23). To minimize this residual, its values at certain points in the element, the so-called integration points or projection points, p, (Fig. 2) will be considered,

$$r_p = N_i(p) A_{ij} \phi_j.$$

Application of the least squares minimum principle demands that the sum of the squares of the residuals of the differential equations at the integration points is minimized. Using the element of Fig. 2, the approximation, ϕ, is continuous at the boundaries of the finite elements. However, using the above-mentioned summation of the squares of the residuals, derivatives are not continuous in the complete domain of interest. As a consequence, restriction is made to first order equations, for which the existence of piecewise continuous first derivatives (and continuity of the function itself) is sufficient to obtain an approximate solution which has, of course, continuous first derivatives [20]. Explicitly written,

$$\int\int_{\Omega} \sum (\text{P.D.E.})^2 \, dV = \sum_E \sum_p w_p r_p^2 = \text{minimum} \tag{24}$$

where Ω is the integration domain, E the element index, and w_p the weighting factor belonging to the integration point, p, of the finite element molecule, E.

The minimum is found by differentiation of equation (24) with respect to the unknowns ϕ_n

$$\sum_E \sum_p w_p N_m(p) A_{mn} N_i(p) A_{ij} \phi_j = 0. \tag{25}$$

Calculation is performed step by step

$$A_k^p = N_s(p) A_{sk};$$
$$E_{ij} = \sum_p w_p A_i^p A_j^p. \tag{26}$$

E_{ij} is the so-called element matrix of the problem. The algorithm (26) can be coded. The corresponding subroutine is called LSFEM (Least Squares Finite Element Method). The least squares procedure of equation (25) is completed by adding the element matrices, E_{ij}, to the global matrix, S_{ij}, in the usual finite-element way

$$S_{ij} = \sum_E E_{ij}. \tag{27}$$

To this global matrix, boundary conditions are added at the appropriate places.

Finally, the choice of the integration points will be mentioned without going into the details of the justification for this choice. For a subdivision in N^2 elements, four integration points are chosen at distances of approximately h/N from the centre of the element, where h is the size of the element (Fig. 2). In this way, the element has an accuracy of $O(h^2)$, and the matrix, S_{ij}, will not be singular.

4. RESULTS AND CONCLUSION

The conclusion of Section 2.2, that the mean flow pattern may be considered as irrotational, will be illustrated with a numerical experiment. For a cylindrically symmetric steady flow without circulation around the axis of symmetry and with uniform inflow and outflow profiles, the streamlines have been calculated. For that purpose, equations (5) and (9) have been transformed to the representation by an approximation matrix (Section 3), and they are solved by the least squares finite element package described in Section 3. Also, the original equations (5) and (12) were solved with the inflow boundary condition $\bar{\omega} = \mathbf{0}$. Since this latter system is non-linear, a generalized Newton iteration procedure was used (ref. [20], Ch. 5.3). For both cases, the results are shown in Figs. 3 and 4. The geometrical data of the tube bank used in this example are presented in Table 1.

Further process data are: shell-side mass flow rate 360 kg s^{-1}, tube-side mass flow rate 256 kg s^{-1}, shell-side inflow temperature 490°C, and tube-side inflow temperature 349°C.

Table 1

Inner shell diameter	0.460 m
Outer shell diameter	0.960 m
Length of tube bank	7.154 m
Height of inflow and outflow openings	0.370 m
Outer tube diameter	0.0210 m
Inner tube diameter	0.0182 m
Pitch (triangular)	0.0270 m
Number of tubes	846

From the numerical results, it turned out that the approximation of the flow field by irrotational flow theory compares with a calculation with the original equations to within a maximum local error of 10% near the edge of the inflow boundary and the outer shell. As a consequence of these two different flow models, the maximum difference in temperature for the two calculations is 7°C, or 5%. This local difference is situated at the connection between lower tube sheet and central tube.

In the following discussion, numerical results will be compared with experimental data. These data have been obtained from a test model of a tube bank with the dimensions described in Table 1. Calculated and measured axial shell-side temperature profiles are shown in Fig. 5, and calculated and measured shell-side

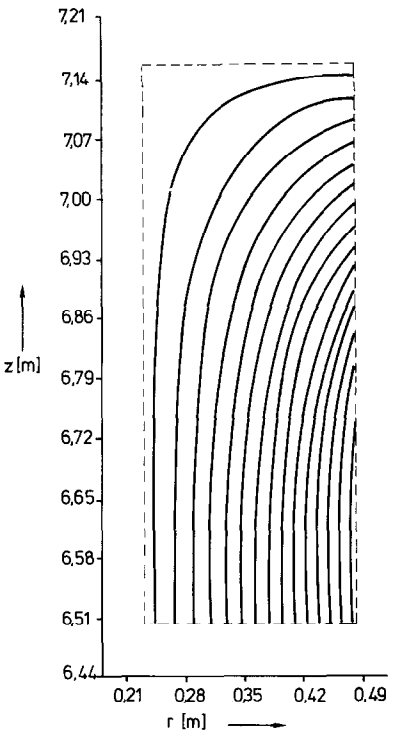

FIG. 3. Shell-side streamlines in inflow region. In calculation with the original equations $R_{\perp} = 34[m^{-4/5}\ s^{-1/5}]$ and $R_{\parallel} = 1.3[m^{-4/5}\ s^{-1/5}]$. Differences between calculation with the original equations and calculation with irrotational flow theory are too small to be visible in the figures.

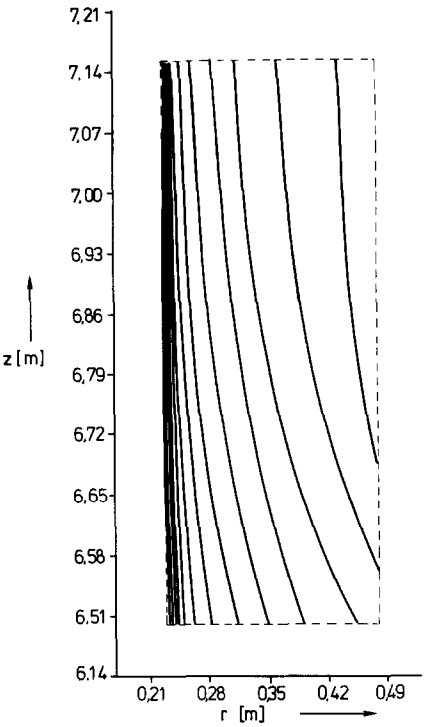

FIG. 4. Shell-side isotherms in inflow region; see also Fig. 3.

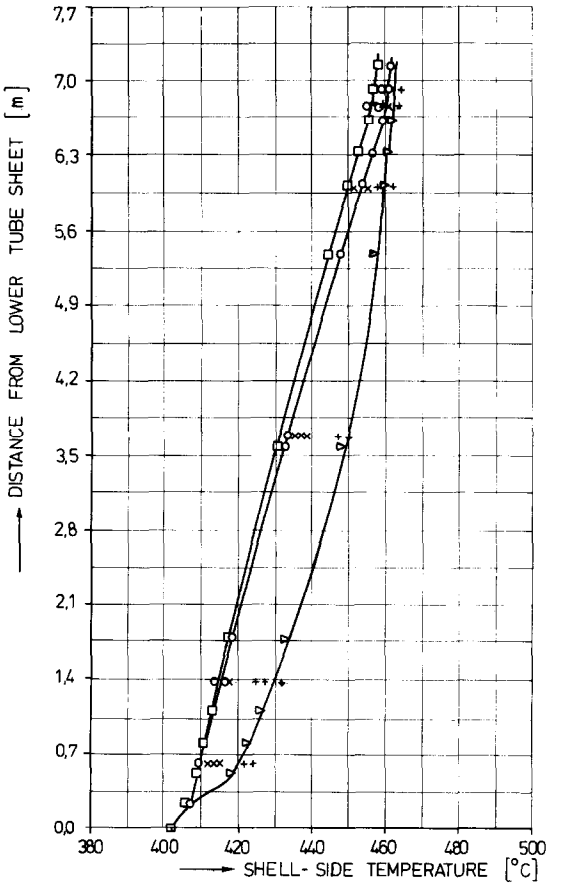

FIG. 5. Shell-side axial temperature. △ calculated values at outer shell, ○ calculated values at centre of shell, □ calculated values at inner shell, + measured values at outer shell, × measured values at centre of shell, ⊕ measured values at inner shell.

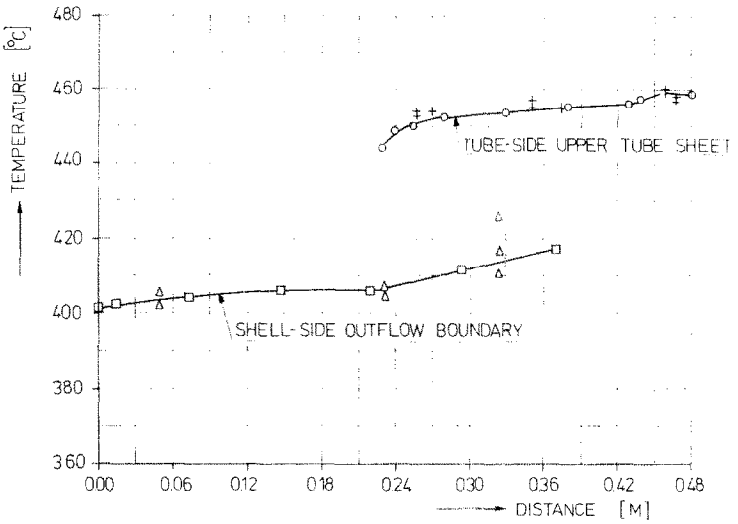

FIG. 6. Calculated and measured shell-side and tube-side outflow temperatures at the same conditions as in Fig. 5.

and tube-side temperatures at the outflow boundaries are shown in Fig. 6.

To account for boundary effects, the shell-side porosity at the outer shell has been increased by a factor of 1.25 over a radial distance of 0.027 m, i.e. in the tube bank, $\gamma = 0.7257$ and near the outer shell, $\gamma = 0.9071$. Further input data are presented in Table 2.

Table 2

Fig.	5 & 6	7	8
Shell-side mass flow rate (kg s^{-1})	281	80	129
Tube-side mass flow rate (kg s^{-1})	267	111	89.4
Shell-side inflow temperature (°C)	461	463	455
Tube-side inflow temperature (°C)	401	344	391

In Fig. 7 it can be observed that, for low values of the shell-side mass flow rate, the description without natural convection is less satisfactory than these for higher mass flow rates. In Fig. 8, rather large temperature differences in the tangential direction account for the scatter in the experimental data. This example shows the limits of a description with axial symmetry and without circulation around the central tube.

Our final conclusion is that the fluid-tube continuum model presented in this paper is a useful and accurate tool for the prediction of the thermal-hydraulic behaviour of shell-and-tube heat exchangers. If only forced convection is considered, the mean flow pattern may be considered to be irrotational, and

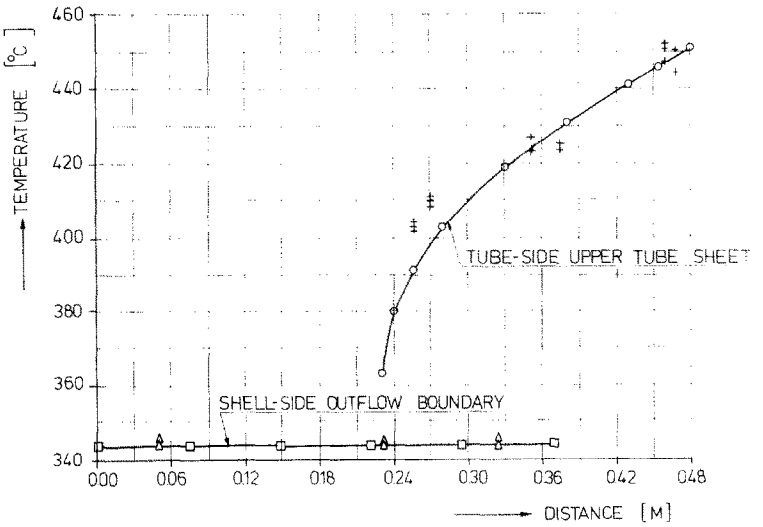

FIG. 7. Calculated and measured shell-side and tube-side outflow temperatures at low shell-side mass flow rates.

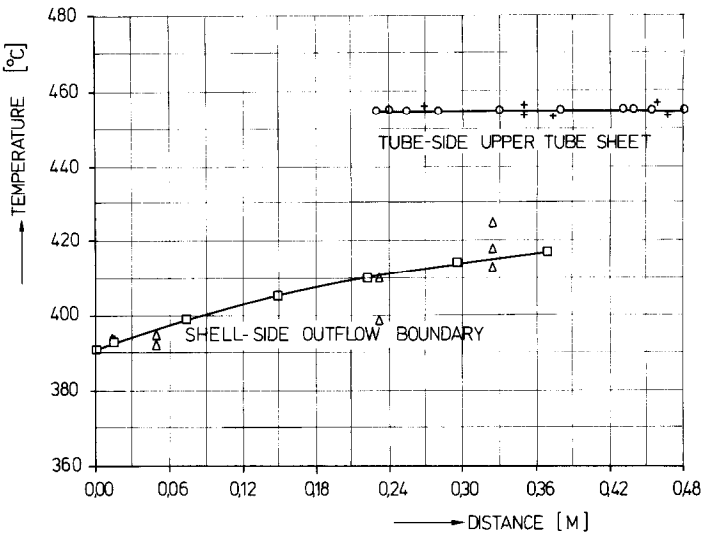

FIG. 8. Calculated and measured shell-side and tube-side outflow temperatures at low tube-side mass flow rates.

consequently only a simple linear system of equations must be solved.

Acknowledgements—The contributions of Dirk van Essen, Cees Hoornweg, Daan Moes, Wim Smits-Schouten and Jan Tulp in the final presentation of this paper are highly appreciated. The present study is part of the Sodium Technology Development Program, and we acknowledge with thanks the financial support of the Netherlands Ministry of Economic Affairs.

REFERENCES

1. M. Shinbrod, *Lectures on Fluid Mechanics*. Gordon and Breach, New York (1973).
2. A. J. Chorin and J. E. Marsden, *A Mathematical Introduction to Fluid Mechanics*. Springer, New York (1979).
3. R. E. Meijer, *Introduction to Mathematical Fluid Dynamics*. Wiley-Interscience, New York (1971).
4. S. V. Patankar and D. B. Spalding, A calculation procedure for the transient and steady-state behaviour of shell-and-tube heat exchangers, in *Heat Exchangers: Design and Theory Sourcebook* (edited by N. Afgan and E. U. Schlünder). McGraw-Hill, New York (1974).
5. T. T. Kao and S. M. Cho, A numerical solution method for the prediction of flow and thermal distribution in shell-and-tube heat exchangers, *Joint ASME/AICHE 18th Nat. Heat Transfer Conf.*, San Diego (1979).
6. W. T. Sha, An overview on rod-bundle thermal-hydraulic analysis, *Nucl. Engng Des.* **62,** 1–24 (1980).
7. H. M. Domanus, V. L. Shah and W. T. Sha, Applications of the Commix code using the porous medium formulation, *Nucl. Engng Des.* **62,** 81–100 (1980).
8. P. M. Morse and H. Feshbach, *Methods of Theoretical Physics*, Ch. 1. McGraw-Hill, New York (1953).
9. H. Lamb, *Hydrodynamics*, Art. 45. Cambridge University Press, London (1974).
10. H. Y. Wong, *Handbook of Essential Formulae and Data on Heat Transfer for Engineers*, Ch. 3.7. Longman, London (1977).
11. C. Truesdell, *The Kinematics of Vorticity*, Indiana University Press, Bloomington (1954).
12. R. B. Bird, W. E. Stewart and E. N. Lightfoot, *Transport Phenomena*. John Wiley, New York (1960).
13. J. G. M. de Bruijn, Least squares finite element solution of a three dimensional flow problem, in *Proc. 3rd Int. Conf. on Finite Elements in Flow Problems*, Vol. 2, pp. 155–165, Banff (1980).
14. J. G. M. de Bruijn and W. Zijl, Least squares finite element solution of several thermal-hydraulic problems in a heat exchanger, in *Proc. 2nd Int. Conf. on Numerical Methods in Thermal Problems*, pp. 752–763, Venice (1981).
15. W. Zijl, Application of numerical approximation methods to the hydrodynamics of vapor and gas bubbles, in *Boiling Phenomena* (edited by S. van Stralen and R. Cole). Hemisphere, Washington (1979).
16. Z. J. Csendes, A finite element method for the general solution of ordinary differential equations, *Int. J. Num. Meth. Engng* **9,** 551–561 (1975).
17. Z. J. Csendes, A Fortran program to generate finite difference formulas, *Int. J. Num. Meth. Engng* **9,** 581–599 (1975).
18. J. M. Boisserie, Generation of two- and three-dimensional finite elements, *Int. J. Num. Meth. Engng* **3,** 327–347 (1971).
19. O. C. Zienkiewicz, *The Finite Element Method*, Ch. 8. McGraw-Hill, London (1977).
20. P. Linz, *Theoretical Numerical Analysis*, Ch. 7. John Wiley, New York (1979).
21. G. K. Batchelor, *An Introduction to Fluid Dynamics*. Cambridge University Press, London (1967).
22. G. C. Everstine, Structural analogies for scalar field problems, *Int. J. Num. Meth. Engng* **17,** 471–476 (1981).
23. P. G. Saffman, Dynamics of vorticity, *J. Fluid Mech.* **106,** 49–58 (1981).

APPENDIX

DERIVATION OF THE FLUID–TUBE CONTINUUM EQUATIONS

The momentum equation

It has already been pointed out that the flow around the tubes is described by the continuity equation (1) and the Navier–Stokes equations (2). Hence, these equations should form the starting point of the derivation of the fluid–tube continuum approximation. Taking the scalar product of equation (2) with $\mathbf{v}$, and integrating over a piece of fluid, $\Omega^*(t)$, with closed boundary, $\partial\Omega^*(t)$, moving with the fluid, results in

(ref. [12], Ch. 3.3)

$$-\iint_{\partial\Omega^*(t)}(p-\rho\mathbf{g}\cdot\mathbf{r})(\mathbf{v}\cdot\mathbf{n})\,\mathrm{d}S^* = \frac{\rho}{2}\frac{\mathrm{d}}{\mathrm{d}t}\iiint_{\Omega^*(t)}(\mathbf{v}\cdot\mathbf{v})\,\mathrm{d}V^* - \eta\iiint_{\Omega^*(t)}\mathbf{v}\cdot\nabla^2\mathbf{v}\,\mathrm{d}V^*. \quad \text{(A1)}$$

The last term of equation (A1) can be split into two parts,

$$-\eta\iiint_{\Omega^*(t)}\mathbf{v}\cdot\nabla^2\mathbf{v}\,\mathrm{d}V^* = 2\eta\iiint_{\Omega^*(t)}\times(\boldsymbol{D}:\boldsymbol{D})\,\mathrm{d}V^* - 2\eta\iint_{\partial\Omega^*(t)}(\mathbf{v}\cdot\boldsymbol{D})\cdot\mathbf{n}\,\mathrm{d}S^* = \phi_v + J_v \quad \text{(A2)}$$

where $\boldsymbol{D} = (\nabla\mathbf{v}+\mathbf{v}\nabla)/2$ is the deformation tensor. The first term on the RHS of equation (A2), ϕ_v, represents the viscous dissipation in the volume $\Omega^*(t)$, and the second term, J_v, represents the rate of viscous energy transport from one piece of fluid to another.

The kinetic energy, T_k, of the fluid volume $\Omega^*(t)$ is given by

$$T_k = \tfrac{1}{2}\iiint_{\Omega^*(t)}(\mathbf{v}\cdot\mathbf{v})\,\mathrm{d}V^*. \quad \text{(A3)}$$

Since on the rigid tube boundaries the no-slip condition, $\mathbf{v} = \mathbf{0}$, holds, the surface integrals in equations (A1) and (A2) have no contribution from these boundaries; only the boundaries with adjacent fluid volumes contribute. This fact makes it possible to consider another volume, Ω, with boundary $\partial\Omega$, not only containing liquid, but also containing tubes. To introduce such a 'fluid–tube mixture', the fluid–tube domain under consideration is divided into subdomains, Ω. These subdomains are sufficiently large to enclose at least one cross-section of a tube. Of course, this partitioning can be done in an infinity of ways, and in Fig. 9 only two possibilities are shown.

It can be proved that the ratio of the two volumes, Ω^*/Ω, is equal to the mean ratio of the two surface areas, $\partial\bar{\Omega}^*/\partial\Omega$, provided that the parts of $\partial\Omega^*$ at the tube walls are not accounted for. For the part of the surface normal to the z-axis this is immediately clear, and in the example of Fig. 9 this ratio is equal to $1-\pi d^2/4ab$. For the part of the surface normal to the x-axis, the surface area not in contact with the tubes is equal to $b\Delta z$ in the configuration of Fig. 9(a), and it is equal to $(b-d)\Delta z$ in the configuration of Fig. 9(b).

An elementary calculation shows that the mean value, $\partial\bar{\Omega}^*$, over an interval of the x-axis with length a, is equal to $(b-\pi d^2/4a)\Delta z$, and this means that the mean value of the ratio of the two surfaces, $\partial\bar{\Omega}^*$ and $\partial\Omega$, is equal to $\partial\bar{\Omega}^*/\partial\Omega = 1-\pi d^2/4ab$. A similar conclusion holds for the mean surface area not in contact with the tubes, normal to the y-axis. As a consequence, it is possible to define infinitesimal volumes, $\mathrm{d}V$, and mean infinitesimal surface areas, $\mathrm{d}S$, in such a way that $\mathrm{d}V/\mathrm{d}V^* = \mathrm{d}S/\mathrm{d}S^* = 1/\gamma$, where γ is the so-called porosity, or mean permeability, defined by $\gamma = \Omega^*/\Omega = \partial\bar{\Omega}^*/\partial\Omega$. In this way, a dilatation of the co-ordinate system is introduced such that the volumes, $\iiint_\Omega \mathrm{d}V$, respectively surface areas, $\iint_{\partial\Omega}\mathrm{d}S$, are equal to the volumes, respectively surface areas of the 'fluid–tube mixture'. The value of the surface integral in equation (A1) depends on the choice of the boundary, $\partial\Omega^*$: different values will be obtained for the configurations of Figs. 9(a) and (b), respectively. From a statistical point of view, it is natural to use the mean value, $\partial\bar{\Omega}^*$, for the part of $\partial\Omega^*$ not in contact with the tubes and, since the part of the surface in contact with the tubes does not contribute to the surface integral, equation (A1) is written as

$$-\iint_{\partial\Omega(t)}(p-\rho\mathbf{g}\cdot\mathbf{r})(\mathbf{v}\cdot\mathbf{n})\gamma\,\mathrm{d}S = \frac{\mathrm{d}T_k}{\mathrm{d}t} + \phi_v + J_v. \quad \text{(A4)}$$

The force, $\mathbf{F}$, applied to the moving fluid–tube element is given by

$$\mathbf{F} = -\iint_{\partial\Omega(t)}(p-\rho\mathbf{g}\cdot\mathbf{r})\mathbf{n}\gamma\,\mathrm{d}S = -\gamma\iiint_{\Omega(t)}\nabla(p-\rho\mathbf{g}\cdot\mathbf{r})\,\mathrm{d}V. \quad \text{(A5)}$$

In equation (A5) use has been made of Gauss's divergence theorem to transform the surface integral into a volume integral in the delated co-ordinate system. Now a mean velocity, $\dot{\mathbf{q}}$, will be defined in such a way that

$$\dot{\mathbf{q}}\cdot\iint(p-\rho\mathbf{g}\cdot\mathbf{r})\mathbf{n}\gamma\,\mathrm{d}S = \iint(p-\rho\mathbf{g}\cdot\mathbf{r})(\mathbf{v}\cdot\mathbf{n})\gamma\,\mathrm{d}S$$

and equation (A4) can be written as

$$\mathbf{F}\cdot\dot{\mathbf{q}} = \frac{\mathrm{d}T_k}{\mathrm{d}t} + \phi_v + J_v. \quad \text{(A6)}$$

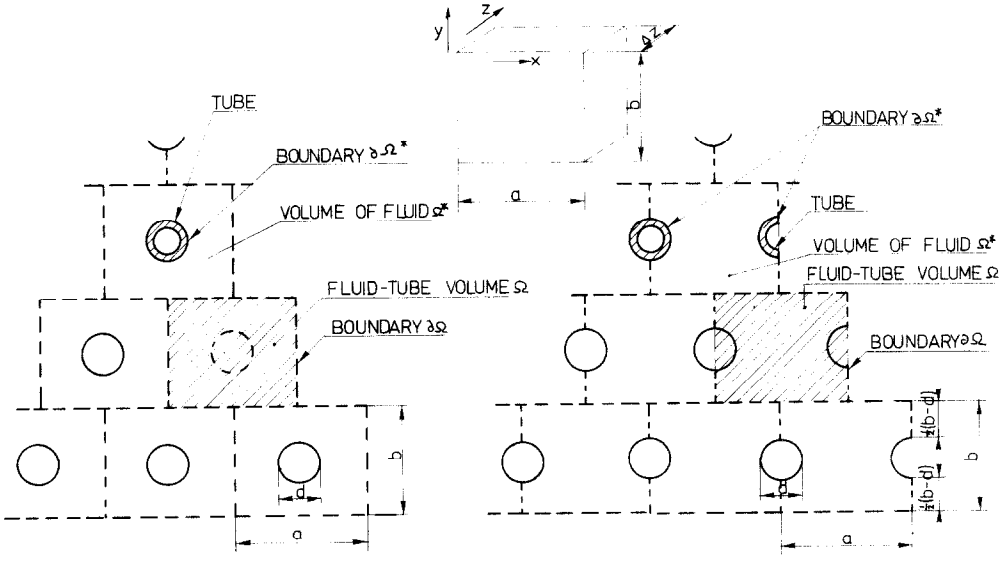

FIG. 9. Subdivision of fluid–tube domain.

Equation (A6) represents an expression for the component of $\mathbf{F}$ in the direction of $\dot{\mathbf{q}}$. If it is possible to express T_k, ϕ_v and J_v in $\dot{\mathbf{q}}$, the component of $\mathbf{F}$ in the direction of $\dot{\mathbf{q}}$ can be determined from equation (A6). Furthermore, if for the components of $\mathbf{F}$ normal to $\dot{\mathbf{q}}$ an additional expression can be obtained, $\mathbf{F}(\dot{\mathbf{q}})$ is known completely. In that case equation (A5) may be considered as the equation of motion in the fluid–tube continuum.

To find the required expressions, the kinetic energy of the moving volume will be related to the mean velocity, $\dot{\mathbf{q}}$, and to a co-ordinate of the moving volume $\mathbf{q}$, defined by

$$\mathbf{q} = \int \dot{\mathbf{q}}(t)\,\mathrm{d}t$$

i.e.

$$T_k = T_k(\mathbf{q}, \dot{\mathbf{q}}).$$

If T_k has a quadratic form, $T_k = \frac{1}{2}m_{ij}(\mathbf{q})\dot{q}_i\dot{q}_j$, where $m_{ij} = m_{ji}$ is a positive definite tensor, and if, in addition, the system were Lagrangian, we would find for $\mathbf{F} = F_i$, $i = 1, 2, 3$,

$$F_i = m_{ij}\ddot{q}_j + \frac{\mathrm{d}m_{ij}}{\mathrm{d}q_k}\dot{q}_k\dot{q}_j - \tfrac{1}{2}\frac{\mathrm{d}m_{kj}}{\mathrm{d}q_i}\dot{q}_k\dot{q}_j. \tag{A7}$$

From equation (A7) it is observed that, for steady rectilinear flow, the force $\mathbf{F}$ depends quadratically on the velocities $\dot{\mathbf{q}}$. From equations (A6) and (A7) it is found that for such a system $\phi_v + J_v = 0$. Also, since m_{ij} does not depend on the flow direction, $\mathrm{d}m_{ij}/\mathrm{d}q_k = 0$ for symmetry reasons and $\mathbf{F} = \boldsymbol{m}\cdot\ddot{\mathbf{q}}$, i.e. there is no force required to maintain a steady flow. This case just describes irrotational flow, which is Lagrangian with a positive definite so-called virtual mass tensor (ref. [9], arts. 135 and 136), where $\nabla^2\mathbf{v} = \mathbf{0}$ (i.e. $\phi_v + J_v = 0$), and where a steady flow has no resistance, provided that some symmetry conditions are satisfied (d'Alembert's paradox, [21]).

For general, not necessarily irrotational, flow, the following expression can be derived from equation (A6):

$$\mathbf{F} = \frac{1}{\dot{q}^2}\left(\frac{\partial T_k}{\partial \dot{\mathbf{q}}}\cdot\ddot{\mathbf{q}}\right)\dot{\mathbf{q}} + \frac{1}{\dot{q}^2}\left(\frac{\partial T_k}{\partial \mathbf{q}}\cdot\dot{\mathbf{q}}\right) \times \dot{\mathbf{q}} - \frac{\dot{\mathbf{q}}\times(\dot{\mathbf{q}}\times\mathbf{F})}{\dot{q}^2} + \frac{(\dot{\phi}_v + J_v)\dot{\mathbf{q}}}{\dot{q}^2}. \tag{A8}$$

The flow in a tube bank is far from irrotational. In general, it will be fully turbulent. From steady-state experiments it is known that, in that case, the force has the direction of the velocity, $\dot{\mathbf{q}}$, and that the form drag,

$$\frac{1}{\dot{q}^2}\left(\frac{\partial T_k}{\partial \mathbf{q}}\cdot\dot{\mathbf{q}}\right)\dot{\mathbf{q}},$$

plus the viscous drag, $(\phi_v + J_v)\dot{\mathbf{q}}$, can be written together in a quadratic form, rather similar to equation (A7) for steady irrotational flow,

$$\mathbf{F} = \frac{1}{\dot{q}^2}\left(\frac{\partial T_k}{\partial q}\cdot\dot{\mathbf{q}}\right)\dot{\mathbf{q}} + \frac{(\phi_v + J_v)\dot{\mathbf{q}}}{\dot{q}^2} = \tfrac{1}{2}k|\dot{\mathbf{q}}|\dot{\mathbf{q}}. \tag{A8a}$$

In equation (A8a), k depends slightly on the magnitude of $\dot{\mathbf{q}}$, and k also depends on the direction of $\dot{\mathbf{q}}$. The form drag is almost zero for flow parallel to the tubes, and the viscous drag is almost negligible with respect to the form drag for flow normal to the tubes.

Since no experimental data are available for the acceleration term,

$$\frac{1}{\dot{q}^2}\left(\frac{\partial T_k}{\partial \dot{\mathbf{q}}}\cdot\ddot{\mathbf{q}}\right)\dot{\mathbf{q}},$$

the expression $\boldsymbol{m}\cdot\ddot{\mathbf{q}}$ from irrotational flow theory will be taken when unsteady flow is considered, thus assuming that an unsteady irrotational flow is superposed to the (non-irrotational) steady flow. In this way the following expression results:

$$\mathbf{F} = \boldsymbol{m}\cdot\ddot{\mathbf{q}} + \tfrac{1}{2}k|\dot{\mathbf{q}}|\dot{\mathbf{q}}. \tag{A9}$$

The values $\boldsymbol{m}$ and k are porportional to the fluid volume, $\gamma\Omega(t)$, under consideration. Consequently, equation (A9) may be written as

$$\frac{\mathbf{F}}{\rho} = -\frac{\gamma}{\rho}\iiint_{\Omega(t)}\nabla(p - \rho\mathbf{g}\cdot\mathbf{r})\,\mathrm{d}V = (\boldsymbol{M}\cdot\ddot{\mathbf{q}} + \tfrac{1}{2}K|\dot{\mathbf{q}}|\dot{\mathbf{q}})\gamma\iiint_{\Omega(t)}\mathrm{d}V \tag{A10}$$

where

$$\boldsymbol{M} = \boldsymbol{m}\Big/\left(\gamma\rho\iiint_{\Omega}\mathrm{d}V\right)$$

and

$$K = k\Big/\left(\gamma\rho\iiint_{\Omega}\mathrm{d}V\right).$$

For N adjacent fluid elements i, $i = 1 \ldots N$, the following expression, from equation (A10), holds:

$$-\frac{1}{\rho}\sum_{i=1}^{N}\iiint_{\Omega_i}\nabla(p - \rho\mathbf{g}\cdot\mathbf{r})\,\mathrm{d}V = \sum_{i=1}^{N}(\boldsymbol{M}_i\cdot\ddot{\mathbf{q}}_i + \tfrac{1}{2}K_i|\dot{\mathbf{q}}_i|\dot{\mathbf{q}}_i)\iiint_{\Omega_i}\mathrm{d}V. \tag{A11}$$

Since the volume elements Ω_i have arbitrary size (but are large enough to contain at least one tube), it is an acceptable approximation to assume continuous functions $\ddot{\mathbf{q}} = \ddot{\mathbf{q}}(\mathbf{r})$, $\dot{\mathbf{q}} = \dot{\mathbf{q}}(\mathbf{r})$, $\boldsymbol{M} = \boldsymbol{M}(\mathbf{r})$, $K = K(\mathbf{r})$ instead of the discrete values $\ddot{\mathbf{q}}_i$, $\dot{\mathbf{q}}_i$, $\mathbf{M}_i$ and K_i. Equation (A11) then becomes

$$\iiint_{\Omega}\frac{1}{\rho}\nabla(p - \rho\mathbf{g}\cdot\mathbf{r})\,\mathrm{d}V = \iiint_{\Omega}(\boldsymbol{M}\cdot\ddot{\mathbf{q}} + \tfrac{1}{2}K|\dot{\mathbf{q}}|\dot{\mathbf{q}})\,\mathrm{d}V \tag{A12}$$

where Ω is any sufficiently large volume. For mathematical convenience, however, the requirement of a minimum volume to make sense for the equation will be dropped, and when replacing $\dot{\mathbf{q}}$ by $\bar{\mathbf{v}}$ and $\ddot{\mathbf{q}}$ by $\mathrm{D}\bar{\mathbf{v}}/\mathrm{D}t$, the following equation is finally found:

$$\boldsymbol{M}\cdot\frac{\mathrm{D}\bar{\mathbf{v}}}{\mathrm{D}t} + \tfrac{1}{2}K|\bar{\mathbf{v}}|\bar{\mathbf{v}} + \nabla\left(\frac{\bar{p}}{\rho} - \mathbf{g}\cdot\mathbf{r}\right) = 0 \tag{A12a}$$

where $\bar{p}$ represents a mean pressure over a sufficiently large volume.

The continuity equation

In a similar way, the continuity equation for another mean velocity, $\langle\mathbf{v}\rangle$, can be derived from equation (1) as follows: equation (1) is equivalent to

$$\iiint_{\Omega^*}\nabla\cdot\mathbf{v}\,\mathrm{d}V^* = \iint_{\partial\Omega^*}(\mathbf{v}\cdot\mathbf{n})\,\mathrm{d}S^* = 0. \tag{A13}$$

The surface integral in equation (A13) has no contribution from the rigid tube boundaries, where $\mathbf{v} = \mathbf{0}$, and, as with the derivation of equation (A4), it is possible to write equation (A13) as

$$\iint_{\partial\Omega}(\mathbf{v}\cdot\mathbf{n})\gamma\,\mathrm{d}S = 0.$$

Now a mean velocity, $\langle\mathbf{v}\rangle$, is defined such that

$$\langle\mathbf{v}\rangle\cdot\iint_{\partial\Omega}\gamma\mathbf{n}\,\mathrm{d}S = \iint_{\partial\Omega}(\mathbf{v}\cdot\mathbf{n})\gamma\,\mathrm{d}S = 0.$$

For N adjacent fluid elements i, $i = 1 \ldots N$, the following

expression holds for the $\langle \mathbf{v} \rangle_i$:

$$\sum_{i=1}^{N} \langle \mathbf{v} \rangle_i \int\int_{\partial\Omega_i} \gamma \mathbf{n} \, dS = 0$$

and again, the discrete values, $\langle \mathbf{v} \rangle_i$, may be replaced by continuous values, $\langle \mathbf{v} \rangle(\mathbf{r})$, resulting in

$$\nabla \cdot [\gamma \langle \mathbf{v} \rangle] = 0. \tag{A14}$$

In this latter expression it is also assumed that $\gamma = \gamma(\mathbf{r})$, thus automatically accounting for regions with different mean porosities. Obviously, $\langle \mathbf{v} \rangle$ represents the volumetric flow rate per unit surface area of the wetted surface (and not of the total 'fluid–tube mixture' surface). Since also $\bar{\mathbf{v}}$ represents a mean velocity related to the wetted surface, it is an acceptable approximation to identify the two mean velocities, i.e. $\langle \mathbf{v} \rangle = \bar{\mathbf{v}}$, and

$$\nabla \cdot (\gamma \bar{\mathbf{v}}) = 0. \tag{A15}$$

The temperature equation

The derivation of the shell-side equation for the mean temperatures, $\bar{T}$, follows almost immediately and will not be considered here in further detail.

The resistance force

Finally, a slight modification of equation (A12) will be proposed: equation (A12) can be written in the form of equation (6) with a force distribution, $\mathbf{Q}$, given by

$$\mathbf{Q} = -\tfrac{1}{2} K |\bar{\mathbf{v}}| \bar{\mathbf{v}} - (\boldsymbol{M} - \boldsymbol{I}) \cdot \frac{\mathrm{D}\bar{\mathbf{v}}}{\mathrm{D}t} \tag{A16}$$

where $\boldsymbol{I}$ is the unit tensor, and

$$\frac{\mathrm{D}\bar{\mathbf{v}}}{\mathrm{D}t} = \frac{\partial \bar{\mathbf{v}}}{\partial t} + \bar{\mathbf{v}} \cdot \nabla \bar{\mathbf{v}}.$$

For irrotational flow parallel to the tubes $\boldsymbol{M} = \boldsymbol{I}$, and for irrotational flow normal to the tubes, $\boldsymbol{M} = M\boldsymbol{I}$, with $M > 1$, since immersion of obstacles in the liquid increases the kinetic energy of the motion with respect to the kinetic energy without these obstacles (see Kelvin's theorem [9]). However, the flow is far from irrotational and, therefore, Kelvin's theorem does not hold. Hence, as an approximation, it will be assumed that for steady flow the term $(\boldsymbol{M} - \boldsymbol{I}) \cdot (\bar{\mathbf{v}} \cdot \nabla \bar{\mathbf{v}})$ is already included in the term $\frac{1}{2} K |\bar{\mathbf{v}}| \bar{\mathbf{v}}$. Consequently, $\mathbf{Q}$ will be given by

$$\mathbf{Q} = -\tfrac{1}{2} K |\bar{\mathbf{v}}| \bar{\mathbf{v}} - (\boldsymbol{M} - \boldsymbol{I}) \cdot \frac{\partial \bar{\mathbf{v}}}{\partial t}. \tag{A17}$$

For unsteady flow, the value of $\boldsymbol{M}$ will be obtained from irrotational flow theory, and in a forthcoming paper, an explicit expression for $\boldsymbol{M}$ will be presented. In this paper restriction will be made steady flows, i.e. $\partial \bar{\mathbf{v}} / \partial t = \mathbf{0}$.

EQUATIONS DU MILIEU CONTINU POUR LA DESCRIPTION DU COMPORTEMENT THERMOHYDRAULIQUE DES ECHANGEURS DE CHALEUR

Résumé — On a étudié le soi disant modèle du "milieu continu tube–fluide" pour la description du comportement thermohydraulique des échangeurs de chaleur, avec une attention spéciale pour la bonne formulation des conditions aux limites. On donne aussi la dérivation des équations à partir des principes de base. Arrivé à un système linéaire d'équations partielles différentielles : l'équation de Laplace et deux équations linéaires de convection, une solution numérique est trouvée avec la méthode des éléments finis basée sur la principe des moindres carrés. Finalement, les résultats numériques sont comparés avec les données obtenues des expériments. Il y a une ressemblance satisfaisante.

KONTINUUMGLEICHUNGEN ZUR BESCHREIBUNG DER THERMOHYDRAULISCHEN FAHIGKEIT VON WARMETAUSCHERN

Zusammenfassung — Der sogenannte Flüssigkeitsrohre Kontinuumansatz, um die thermohydraulische Fähigkeit von Wärmetauschern beschreiben zu können, wird kritisch betrachtet. Insbesondere ist die korrekte Formulierung der Randbedingungen beachtet worden und ist auch eine Herleitung der Gleichungen, ausgehend von der Grundprinzipien, presentiert worden. Das resultierende System gekuppelter partieller Differentialgleichungen : eine Laplacesche Gleichung and zwei lineare konvektive Gleichungen, ist numerisch gelöst worden mit einer finiten Elementenverfahren, basierend auf einem kleinsten Quadraten Minimumprinzip. Schliesslich sind die numerischen Resultate mit den experimentellen Daten verglichen worden. Die Übereinstimmung ist gut.

ИСПОЛЬЗОВАНИЕ УРАВНЕНИЙ СПЛОШНОЙ СРЕДЫ ДЛЯ РАСЧЕТА ОБТЕКАНИЯ КОЖУХА И ПРОФИЛЕЙ ТЕМПЕРАТУР В ТЕПЛООБМЕННИКАХ

Аннотация — Дан критический обзор так называемого метода сплошной среды, используемого для описания термогидравлического режима работы теплообменников. Особое внимание уделено корректной формулировке граничных условий. Дан вывод основных уравнений. Полученная в результате линейная система дифференциальных уравнений в частных производных уравнение Лапласа и два линейных уравнения конвекции – решена численно методом конечных элементов, основанном на принципе минимума наименьших квадратов. И наконец, проведено сравнение численных результатов с экспериментальными данными и получено их хорошее совпадение.